VIIRS SDR Algorithm Three-Phase Performance Test Approach for Radiometric Calibration

Stephen Mills*, Lushalan Liao, Tohru Ohnuki, Frank Sun

Northrop Grumman Aerospace Systems

* Contact: stephen.mills@ngc.com; phone: (310)813-6397

Introduction

The Visible Infrared Imager Radiometer Suite (VIIRS) is part of the NPOESS Preparatory Project (NPP). Northrop Grumman Corporation (NGC) took a unique three-phase approach to testing the SDR radiometric performance. The approach was dictated by the progress of the sensor testing and the SDR algorithm development. The synergy of testing the SDR algorithm with both a sensor model and with test data produces an understanding that neither one alone can produce.

The Three Phases of Algorithm Testing

1. In the first phase NGC developed a sensor model and produced look-up tables (LUT) consistent with the model. This was necessary because complete characterization was not yet available. It did demonstrate consistency between model and SDR Algorithm.
2. In the second phase we used the actual raw data from the sensor testing and characterization as input into the SDR. The LUT were produced from characterization. This had the advantage of being most consistent with actual sensor, but by itself is limited by the limitations of the tests. It also does not involve the model at all.
3. The third phase was to develop sensor model from same characterization data used to produce SDR LUT. By itself this potentially has a problem in that a mistake in both would be masked by a consistent, but wrong result. It did, however, demonstrate consistency between model and SDR Algorithm.

How 3 Phase Method Validates

This 3 phase process validates to a certain level both the SDR algorithm and the sensor model and guarantees consistency between the theory that the SDR algorithm is based, and the algorithm as programmed. Comparing the results from each phase resolves the limitations inherent in each. The logic is that if as-built sensor is consistent with SDR algorithm, and if SDR algorithm is consistent with as-built sensor model, then as-built sensor is consistent with as-built sensor model.

We have completed the 3 phases of test and have shown that the SDR algorithm and sensor model are consistent with the as-built sensor. By comparing with SDR performance predictions based on analysis outside of the actual SDR tests, confidence is shown between how the SDR should theoretically perform, and how the actual algorithm as programmed performs.

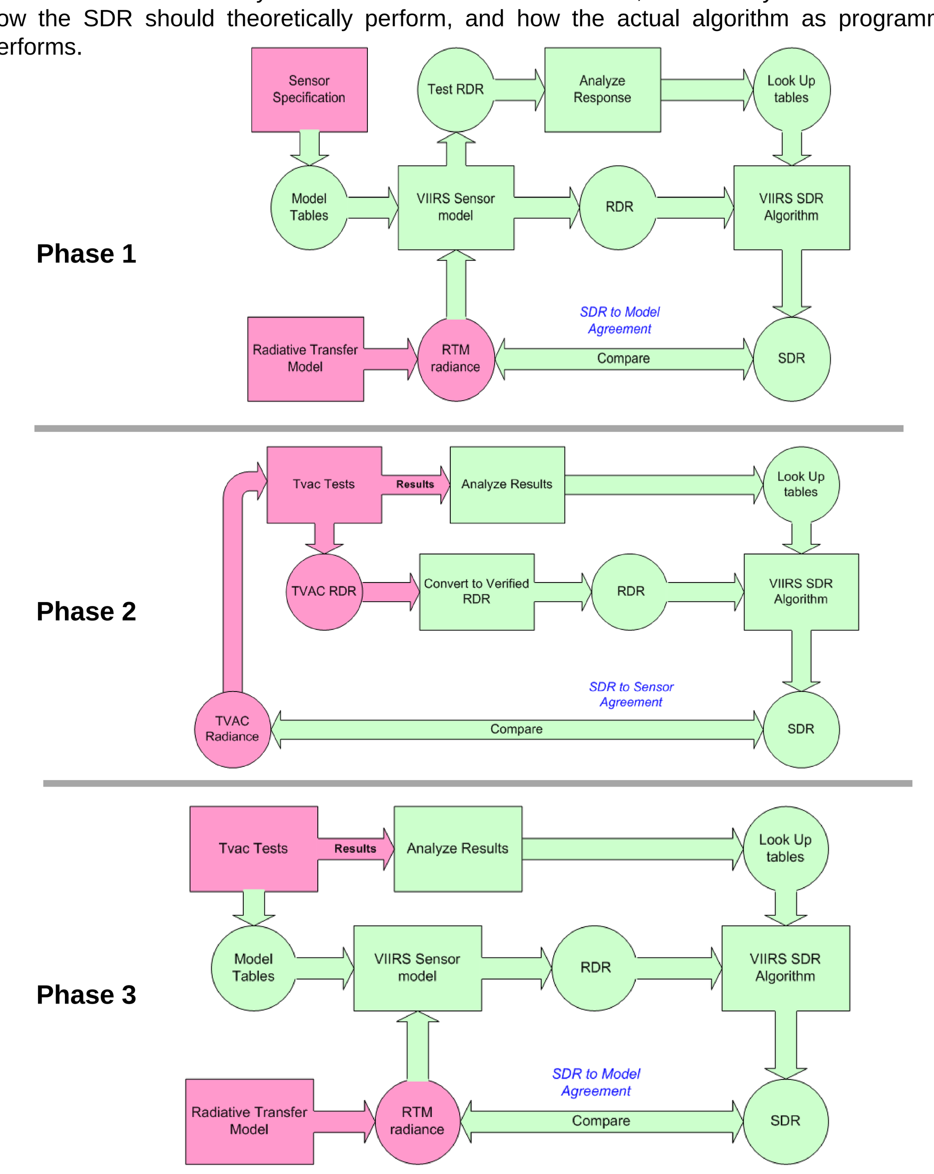

Science, Sensor & Software (S^3)

SDR performance can be with respect to three different points-of-view. These are science, sensor and software (SSS or S^3).

1. Science" here refers to the use scientific or engineering theory to understand how the sensor should work, even before it is built. In fact, the design is based on these principles. The scientifically based theory is described in the Algorithm Theoretical Basis Document (ATBD).
2. "Sensor" here refers to the actual as-built sensor. This includes how it is characterized before launch– its measurement uncertainty and its response to various stimulus.
3. "Software" here refers to the actual software of the SDR. The theory in the ATBD is used to produce a working algorithm. In addition to implementing the algorithms described in the ATBD, software must incorporate raw data formats, thermal and temporal interpolation methods, quality flags for missing or corrupted data, and so forth.

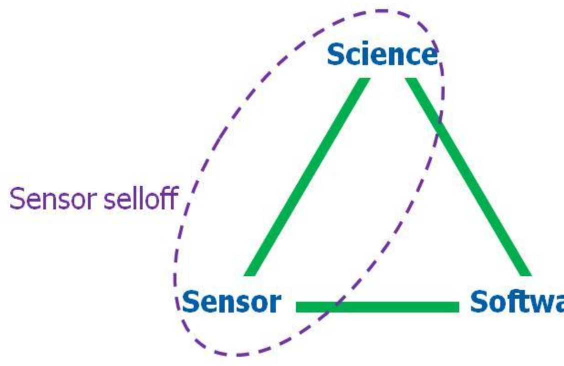

S^3 Perspective on Testing the Calibration Algorithm

With the S^3 in mind, the performance predictions presented here are considered from 3 different perspectives:

1. VIIRS sensor vendor (Raytheon) performance predictions & allocations.
2. Northrop Grumman Corporation (NGC) error budget predictions & allocations.
3. NGC sensor model predictions.

The purpose of each of these will be considered and contrasted with the other 2.

Performance predictions by the VIIRS sensor vendor are primarily for the purpose of demonstrating adequate performance against the VIIRS Sensor Spec. The sensor spec is often defined so as to specify requirements at some of the extremes of the performance envelope. For example, it specifies noise and many other performance parameters at the end-of-scan, which is where it is the highest. Stray light and crosstalk are specified with respect to high contrast situations that are actually rare when viewing actual scenes on the Earth.

Phase 2 - Performance Verification Using Thermal Vacuum (TVAC) Test Data

TVAC test data is the best pre-launch "real" instrument data available. It represents the characteristics of the NPP VIIRS instrument that may not be fully simulated by models or represented by global synthetic and proxy data. It also provides flat uniform target scenes that can be used to calibrate the instrument across HAM sides and detectors, an opportunity hard to find on orbit because uniform earth scene are rare. This study provides a comprehensive understanding of the performance of the SDR algorithm and LUT. The results of this analysis can be leveraged to supplement post-launch on-orbit Cal/Val analysis.

SDR performance verification using TVAC test data has the following limits:

- Most TVAC data is taken in diagnostic mode, but the SDR algorithm is designed to process only the operational mode RDR.
- The TVAC data does not provide for a calibrated illumination of the SD, which means that Reflective band gain calibration can't be performed
- Nevertheless, it does provide one of the 3 elements in S^3, and provides the ability to compare sensor model SDR outputs with actual TVAC results.

The following considerations were made for data selection:

1. Ideally, data would be selected from tests performed in operational mode (similar to on-orbit retrievals), that is data selected from diagnostic mode replicated to match the dimensions associated with operational mode.
2. Include tests that cover the dynamic range of all bands.

Day-in-the Life test data was selected to meet the first requirement. RC-02 test data was selected to satisfy the dynamic range of reflective bands and RC-05 was selected for emissive bands. RC-02 and RC-05 tests are in diagnostic mode. The Earth View Data needed to be replicated to match the dimensions of the operational mode.

Day-in-the-Life Testing

The Day in the Life (DitL) test examined the VIIRS sensor performance during typical on-orbit behavior. Part 1 corresponds to the First Day in the Life of the VIIRS instrument and Part 2 corresponds to the Standard Day in the Life. The DitL test is one of the few TVAC tests that runs with VIIRS in operational mode. Only one SIS100 Radiance level is used during the test. Below is a typical example of a DitL granule (48 scans) after calibration.

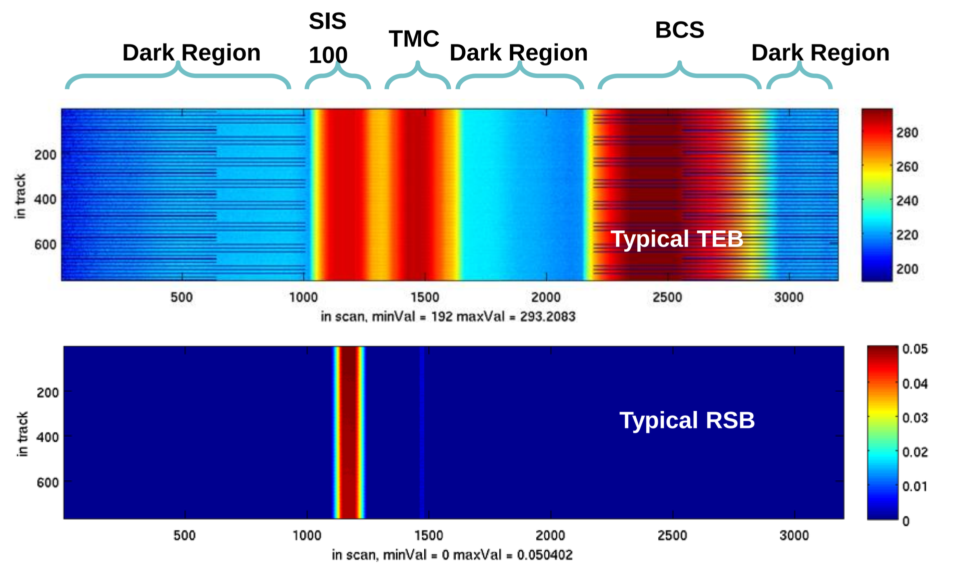

A concern with testing the SDR algorithm only with simulated proxy data is that this does not prove that the algorithm is properly interpreting the data formats, and testing the algorithm with the DitL data proves that the data is being properly interpreted.

The following shows radiometric performance from the VIIRS SDR Algorithm software running on the DitL tests. The emissive bands are accurate to within 10 mK, and much of this could be calibration source uncertainty. For the reflective bands the calibration source is only known to within 10%, and for the DitL radiance level 5 bands saturate. Given these facts, the Calibration performs as expected.

Band	Center Wavelength (nm)	BCS BT (K)	TVAC-based LUTs
M12	3700	292.369	292.3774
M13	4050	292.369	292.3579
M14	8550	292.369	292.3024
M15	10763	292.369	292.2959
M16	12013	292.369	292.3144
I4	3740	292.369	292.3654
I5	11450	292.369	292.2959

Band	Center WL (nm)	SIS-100 Radiance	SIS-100 Radiance After Window	TVAC-based LUTs
M1	412	20	18.6	19.499
M2	445	39.6	36.8676	37.662
M3	488	75.3	70.15701	74.971
M4	555	148.7	136.431	140.062
M5	672	266.5	247.845	259.411
M6	746	319.1	296.763	38.257
M7	865	338.8	315.084	343.656
M8	1240	276.4	259.816	
M9	1378	183.2	128.24	
M10	1610	137.9	129.826	
M11	2250	35.3	10.237	10.406
I1	640	231.7	215.481	227.809
I2	865	338.8	315.084	347.12
I3	1610	137.9	129.626	77.626

Thermal Emissive band Calibration Testing Using RC-05 TVAC Data

There are 2 aspects of the RC-05 data that complicate construction of the Raw data record (RDR): The RC-05 test is performed in Diagnostic Mode, whereas the SDR calibration code is designed to only operate on operational RDR data. In diagnostic mode, the data is not EV aggregated for the single gain bands, and does not cover the full scan. There are 2048 samples in the MOD bands & twice as many in the IMG bands, and these are repeated 3.07 times to produce a full scan of unaggregated data. This is then aggregated for the MOD and IMG single gain bands to simulate an operational VRDR. The BB cal source is carefully centered to correspond to the actual scan angle so that the RVS will be properly aligned with the appropriate scan angles. The statistics provided here are taken over 30 samples centered at the BCS. This limited region was chosen to minimize non-uniformities from the calibration source. It should be noted that averages are taken per detector, per HAM side over the 24 scans for each side.

In the TVAC data used from RC-05 there were a total of 30 collects used here representing 10 Blackbody Calibration Source (BCS) radiance levels from the 3 plateaus - cold, nominal and hot. The 10 BCS brightness temperatures used here are between approximately 190 K and 340 K. The analysis of the SDR algorithm output showed that for all radiances levels the noise and radiometric requirements were met with the exception of one detector for M12 at the 230 K only.

Noise Results of Thermal Emissive Bands

The figures show examples of the noise for the same bands in terms of NEdT and BCS Temperature. In these plots the spread in NEdT over all the detectors is shown by error bars. Note that these are not standard deviations, but instead describe the range from lowest to highest detector. The NEdT requirement is shown as an orange bar on these plots, except in cases where it is off the plot, and is indicated with an arrow and a note.

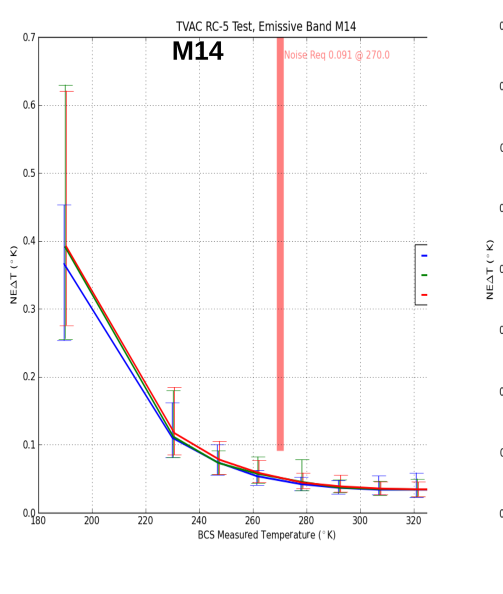

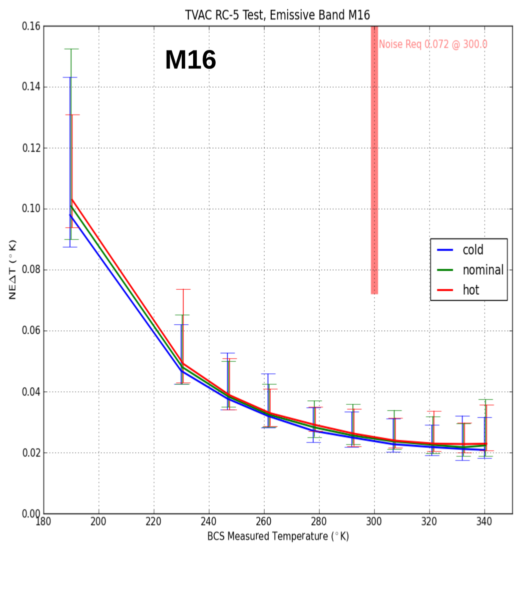

Radiometric Error for Emissive Bands Relative to Requirements

The following figures show the relative radiometric error versus brightness temperature. This is the most convenient way to compare the performance with the requirements, which are spec'ed to these. The error bars show the entire spread over the detectors and mirror side from lowest to highest. Again, the bars are slightly shifted horizontally for clarity. It can be seen for M12 that the error bar extends into the orange requirement gate from detector 1.

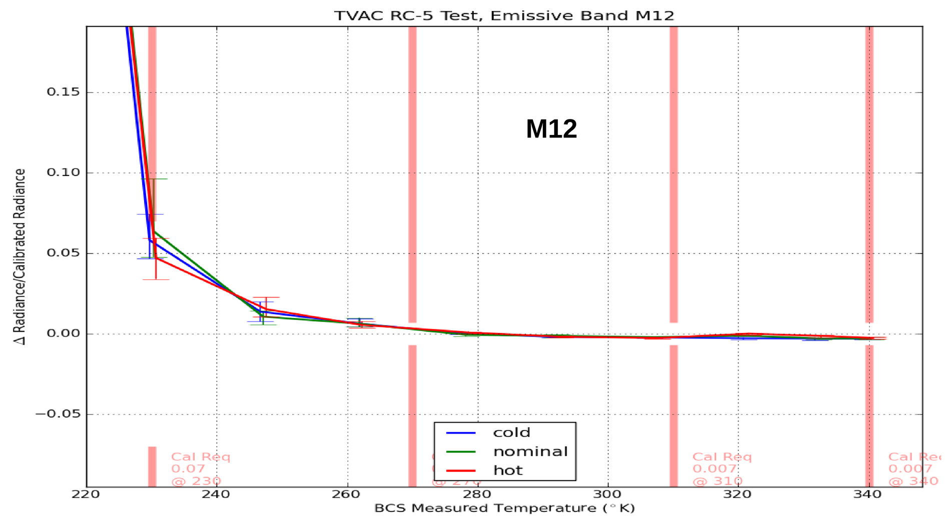

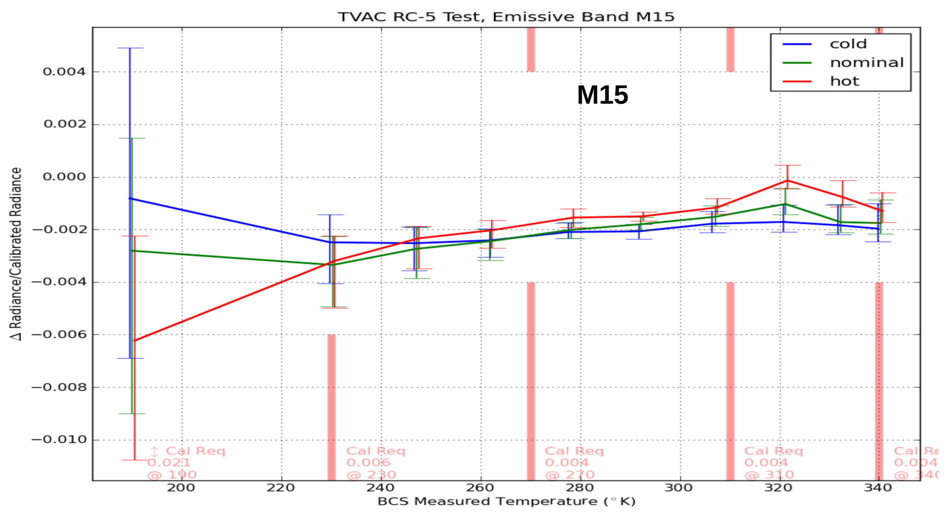

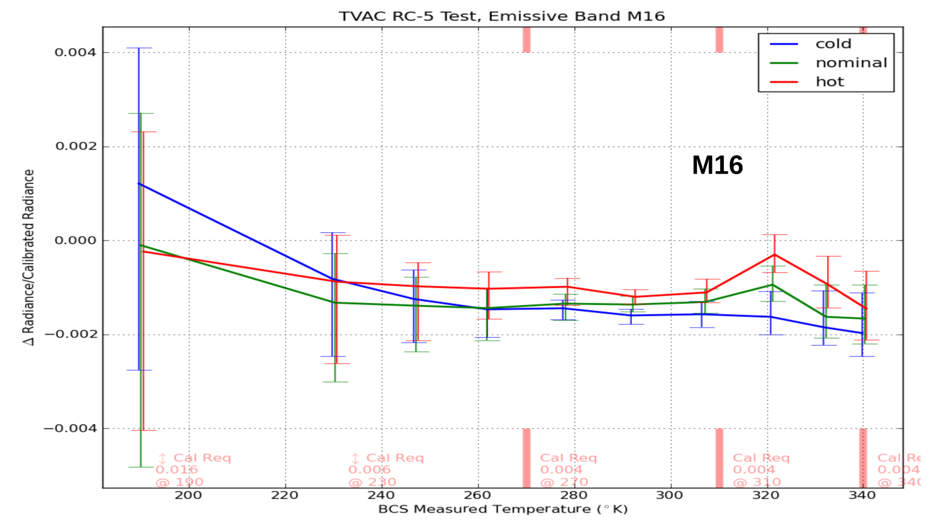

Radiometric Error for Reflective Bands

The purpose of the reflective calibration coefficients is to convert instrument digital number to radiance. It is assumed that the instrument response to the at focal-plane radiance can be described by a quadratic function. Calibration for the reflective band was performed at three plateaus. Thus three sets of coefficients were produced from the RC2 tests.

Traditionally, calibration accuracy is transferred from a laboratory standard to an instrument. Thus, an instrument can never achieve higher accuracy than what the knowledge of the laboratory standard is. This present a problem for reflective band calibration for VIIRS since the requirement of 2% total uncertainty is more stringent than the available accuracy of laboratory standards commonly employed in reflective radiometric calibration. In particular our laboratory standard, SIS-100, can be expected to have uncertainty on the order of 5%. Thus, the usual approach of transferring accuracy of the laboratory standard to the instrument is insufficient for our purpose. Instead, a differential technique which takes advantage of the temporal stability of the source is employed. This technique allows one to determine the ratios of the quadratic (c_2) and offset (c_0) terms over the scale (c_1) in the calibration equation accurately. In fact, the majority of the uncertainty comes from the knowledge of the tie-point radiance. The uncertainty arising from the characterization of the coefficient ratios is small compared to the tie-point uncertainty due to the characterization uncertainty of the reflectance of the solar diffuser. The rest of this document shows the radiance uncertainty as a result of the uncertainty of the calibration coefficient ratios.

The datasets used in the coefficient retrievals come from the RC2 tests conductive during environmental testing of the sensor. Not all collects were used for all bands. Data screening for saturation effects and anomalous data resulted in a reduced data set. Some examples of the results are shown below.

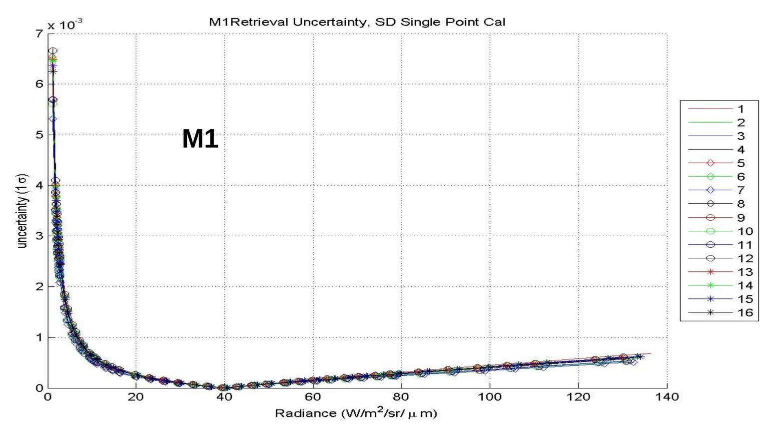

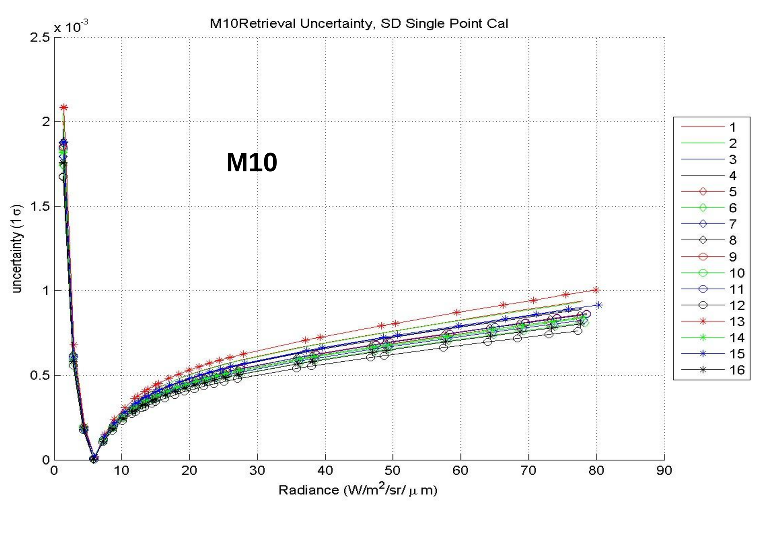

Phase 3: Model Based Results

For the determination of radiometric calibration, the VIIRS sensor model was run on NPP Proxy remapped MODIS granules. The images below show a 48 scan granule of radiances for a reflective and emissive band. Several selected granules from two orbits of MODIS data were processed using the model F 1030h orbit parameters and calibrated with the lookup tables produced from TVAC tests. A calibration correction factor computed using the solar diffuser calibration code was used as this correction would be present in real operation.

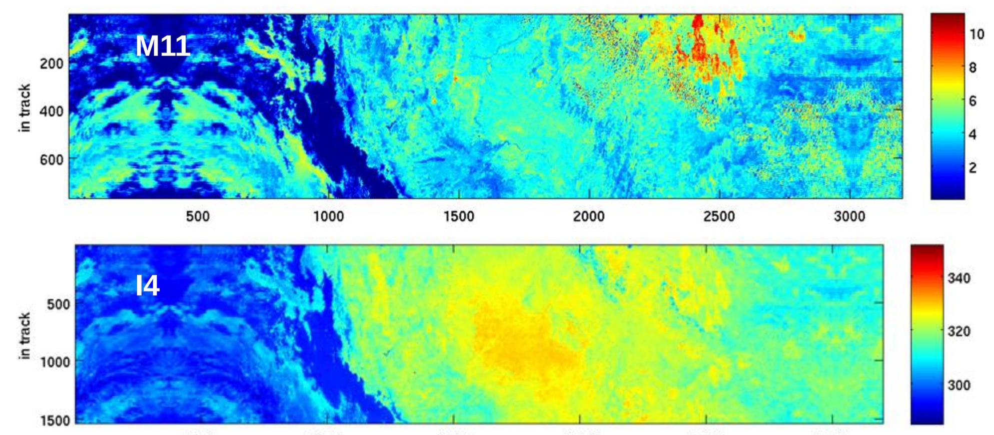

The radiances were input into the model to produce simulated raw data counts. The counts were then input into the SDR calibration algorithm to produce a retrieve radiance. The radiance were then compared with the "truth" radiance scenes. The results are presented in the following plots. Each band is plotted twice, the top scatter plot has sensor input radiance on the x-axis, the calibrated output minus the input on the y-axis. An error in calibration would manifest as a tilt in the response or an offset. The slope and offset of a first order fit are reported below the top plot. The bottom plot shows the data binned and scaled with the error bar being the standard deviation of the scaled data in each bin. A shift up or down represents a gain error, a curve in the response represents a non-linearity. The accuracy and noise requirements are presented as red 'gates' and the magenta 'I' bar respectively. Lmin and Lmax for each band are also shown in green as is the low gain to high gain transition.

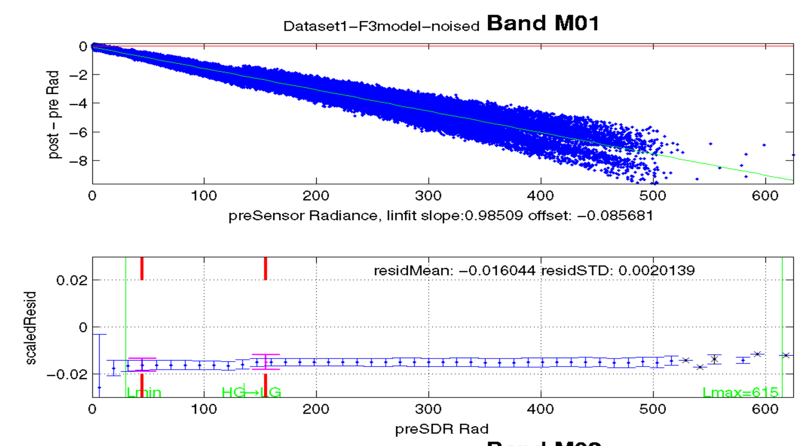

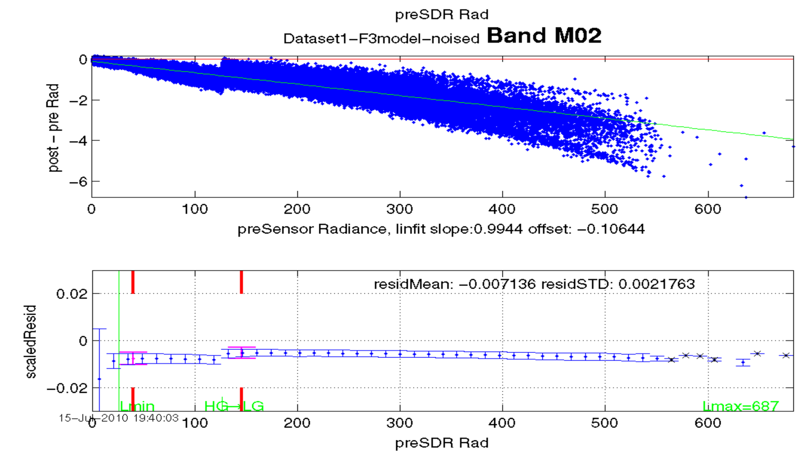

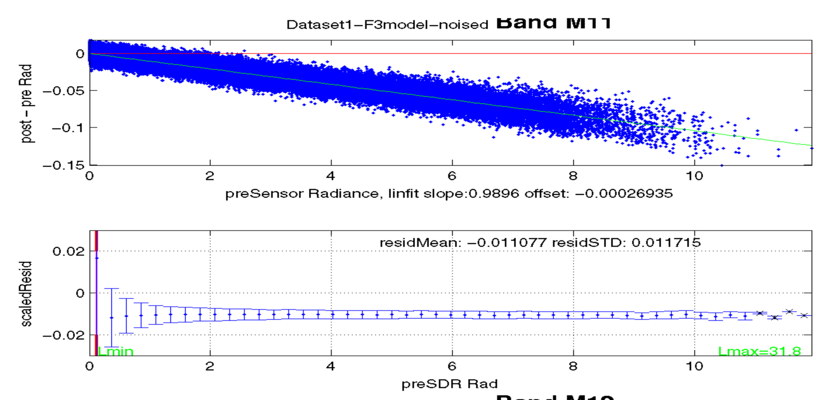

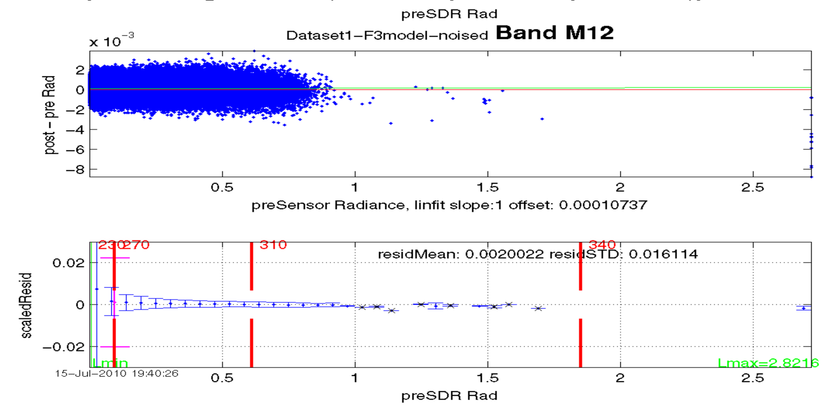

Band	High Gain or Single Gain				LmaxHG≅LminLG	Low Gain			
	Lmin	Ltyp	50% Lmax	90% Lmax		Lmin	Ltyp	Lmax/2	90% Lmax
M1	-0.0166	-0.0164	-0.0162	-0.0165	-0.0160	-0.0151	-0.0151	-0.0153	No data
M2	-0.0087	-0.0080	-0.0078	-0.0082	-0.0057	-0.0054	-0.0061	-0.0075	No data
M3	-0.0116	-0.0117	-0.0119	-0.0124	-0.0125	-0.0126	-0.0147	-0.0174	-0.0176
M4	-0.0123	-0.0122	-0.0127	-0.0135	-0.0135	-0.0125	-0.0126	-0.0130	No data
M5	-0.0071	-0.0071	-0.0086	-0.0094	-0.0085	-0.0085	-0.0080	No data	No data
M6	-0.0091	-0.0083	-0.0080	-0.0080	-0.0080	NA	NA	NA	NA
M7	-0.0102	-0.0102	-0.0064	-0.0088	-0.0085	-0.0085	-0.0099	-0.0109	No data
M8	-0.0140	-0.0125	-0.0130	No data	No data	NA	NA	NA	NA
M9	0.0093	-0.0103	-0.0097	-0.0105	No data	NA	NA	NA	NA
M10	-0.0141	-0.0105	-0.0112	No data	No data	NA	NA	NA	NA
M11	0.0113	No data	No data	No data	No data	NA	NA	NA	NA
I1	-0.0231	-0.0124	-0.0112	No data	No data	NA	NA	NA	NA
I2	-0.0096	-0.0081	-0.0082	-0.0085	-0.0100	NA	NA	NA	NA
I3	-0.0315	-0.0086	-0.0006	No data	No data	NA	NA	NA	NA

Thermal Emissive Band fractional error base on model

Band	Lmin	Ltyp	190K	230K	270K	310K	340K
M12	0.0056	0.0014		0.0056	0.0014	0.0001	No data
M13	0.0172	0.0011		0.0172	0.0034	0.0005	No data
M14	-0.1834	-0.0129	-0.1834	-0.0307	-0.0129	0.0124	No data
M15	-0.0763	0.0031	-0.0763	-0.0117	-0.0036	0.0046	No data
M16	-0.0266	0.0034	-0.0266	-0.0048	-0.0006	0.0049	No data
I4	0.0217	-0.0010		0.0217	-0.0010	-0.0063	No data
I5	0.0270	0.0131	0.0270	0.0028	0.0040	0.0045	No data

AMS 2011 #652